

## Supplemental Data

### A Specialized Vascular Niche for Adult Neural Stem Cells

Masoud Tavazoie, Lieven Van der Veken, Violeta Silva-Vargas,  
Marjorie Louissaint, Lucrezia Colonna, Bushra Zaidi,  
Jose-Manuel Garcia-Verdugo, and Fiona Doetsch

#### Supplemental Experimental Procedures

##### Immunostaining

Whole mounts were immunostained as described (Doetsch and Alvarez-Buylla, 1996). Whole mounts for laminin were only fixed 6 hours. For BrdU and MCM2, whole mounts were sequentially incubated in methanol and acetone prior to immunostaining (Doetsch and Alvarez-Buylla, 1996). All other immunostainings were performed without methanol and acetone. The following primary antibodies were used: CD31 (rat 1:500; BD Pharmingen), Ki67 (rabbit 1:1000; Novocastra), GFP (rabbit 1:1000; Invitrogen), GFP (mouse 1:1000; Molecular Probes), EGFR (sheep 1:50; Upstate), Mash1 (mouse 1:50; kind gift of Jane Johnson), AQP4 (rabbit 1:250; Chemicon), AQP4 (mouse 1:100; Abcam), Doublecortin (guinea pig 1:300; Chemicon), Laminin (rabbit 1:1000; Sigma), NG2 (rabbit 1:250; Chemicon), MCM2 (goat 1:1000; Santa Cruz), SMA (mouse 1:1000; Sigma), Sox2 (rabbit 1:250; Chemicon), PSA-NCAM (mouse 1:500; Chemicon), S100b (mouse 1:100; Sigma), NeuN (mouse 1:250; Chemicon), GFAP (guinea pig 1:500; Advanced Immunochemicals INC.), ZO-1 (rabbit 1:100; Invitrogen), Occludin (rabbit 1:100; Invitrogen). Blocking solutions were 10% donkey serum (Jackson Immuno) in PBS/0.5% Triton X-100 (Sigma) for CD31, GFP, Mash1, doublecortin, NG2, MCM2,

SMA, Sox-2, PSA-NCAM, S100b, NeuN, GFAP, ZO-1 and Occludin; PBS/0.1%Triton X-100 for AQP-4 and laminin, or PBS alone for EGFR. For ZO-1 and Occludin staining, whole-mounts were pre-treated in protease type XIV (Sigma) for 10 minutes at 37 °C prior to blocking. TUNEL staining was done using the *In situ* Cell Death Detection Kit (Roche). Whole-mounts were revealed with secondary antibodies (Jackson Immuno) and imaged using a Zeiss LSM510 confocal microscope. For SMA, AQP-4 and NG2 immunostaining in sections, 40 µm frontal sections were cut on a vibratome, and immunostaining performed as described above. All immunostainings were done in triplicate.

### **Supplemental Reference**

Doetsch, F., and Alvarez-Buylla, A. (1996). Network of tangential pathways for neuronal migration in adult mammalian brain. *Proceedings of the National Academy of Sciences of the United States of America* 93, 14895-14900.

## Supplemental Figures

### Supplementary Figure 1

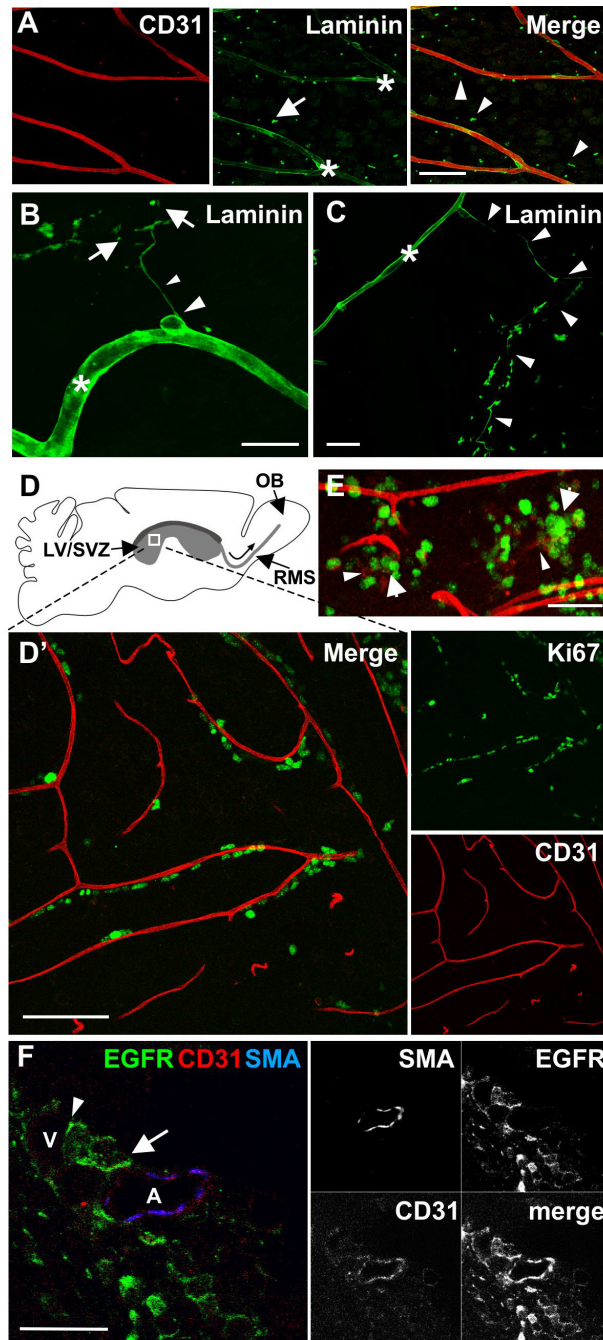


**Figure S1.** Characterization of SVZ blood vessels and their association with dividing cells. (A-C) A laminin-rich basal lamina surrounds SVZ blood vessels. (A) Z-stack projection of whole-mount SVZ immunostained with antibodies against CD31 and

laminin. Blood vessels in the SVZ (red) are ensheathed by a basal lamina (green, asterisks in A, B and C), which exhibits some heterogeneity in intensity of staining. Laminin immunoreactive dots (arrow, central panel, arrowheads, right panel) are scattered over the wall of the ventricle. (B) In some areas of the SVZ, the entire structure of basal lamina fractones extending from blood vessels can be visualized. Here, the long stem (small arrowhead), bulbs (arrows), and base (large arrowhead) of a basal lamina fractone are shown. Note that the bases of fractones frequently arise from perivascular cells. (C) Occasionally, the stems of fractones extend for extremely long distances (small arrowheads). (D, E) Dividing cells lie adjacent to blood vessels throughout the SVZ. (D) Schema showing a sagittal view of the entire lateral ventricle, with a box representing the caudal area of the SVZ depicted in the confocal image below (D'). Dividing cells (green) are closely associated with blood vessels (red) in the caudal SVZ, as seen in the anterior horn (Figure 1). (E) Frequently, clusters of dividing cells (arrows) that are not associated with longitudinal vessels of the SVZ plexus, are associated with blood vessels (arrowheads) that loop into the SVZ from the underlying striatum. These vessels are difficult to visualize in their entirety, as the antibodies do not penetrate deeply into the tissue. (F) EGFR positive cells (green) are found adjacent to both SMA positive (blue) presumptive arteries ("A") (arrow) and SMA negative vessels ("V") (arrowhead). Only a few SMA positive vessels were present in the SVZ, which primarily contains capillaries. Scale bars: (A, E) 50  $\mu\text{m}$ , (B, C, F) 20  $\mu\text{m}$ , (D) 100  $\mu\text{m}$ .

**Supplementary Figure 2**

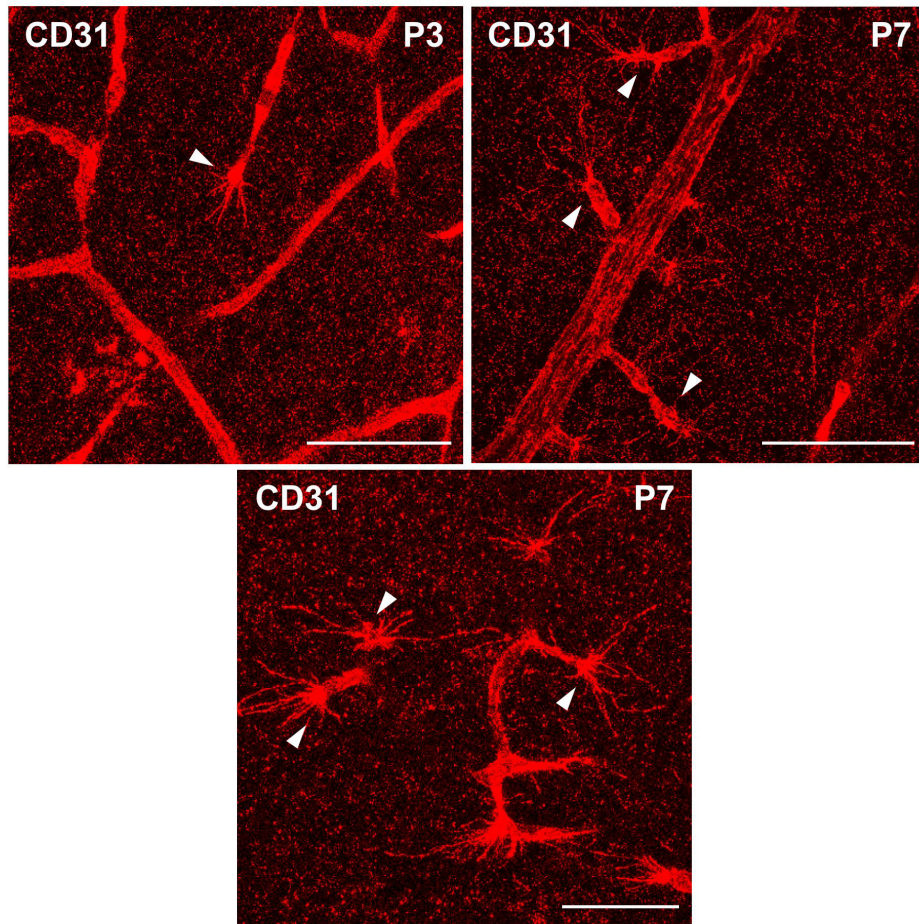


**Figure S2.** Angiogenesis in the perinatal SVZ. Confocal images showing the formation of new blood vessels in the SVZ vascular plexus at postnatal day 3 (P3) and postnatal day 7 (P7). CD31 positive endothelial tips cells (arrowheads) have numerous filopodia, and comprise the leading edge of developing blood vessels. Tip cells were not observed in the adult SVZ. Scale bars: 50  $\mu$ m.

Supplementary Figure 3

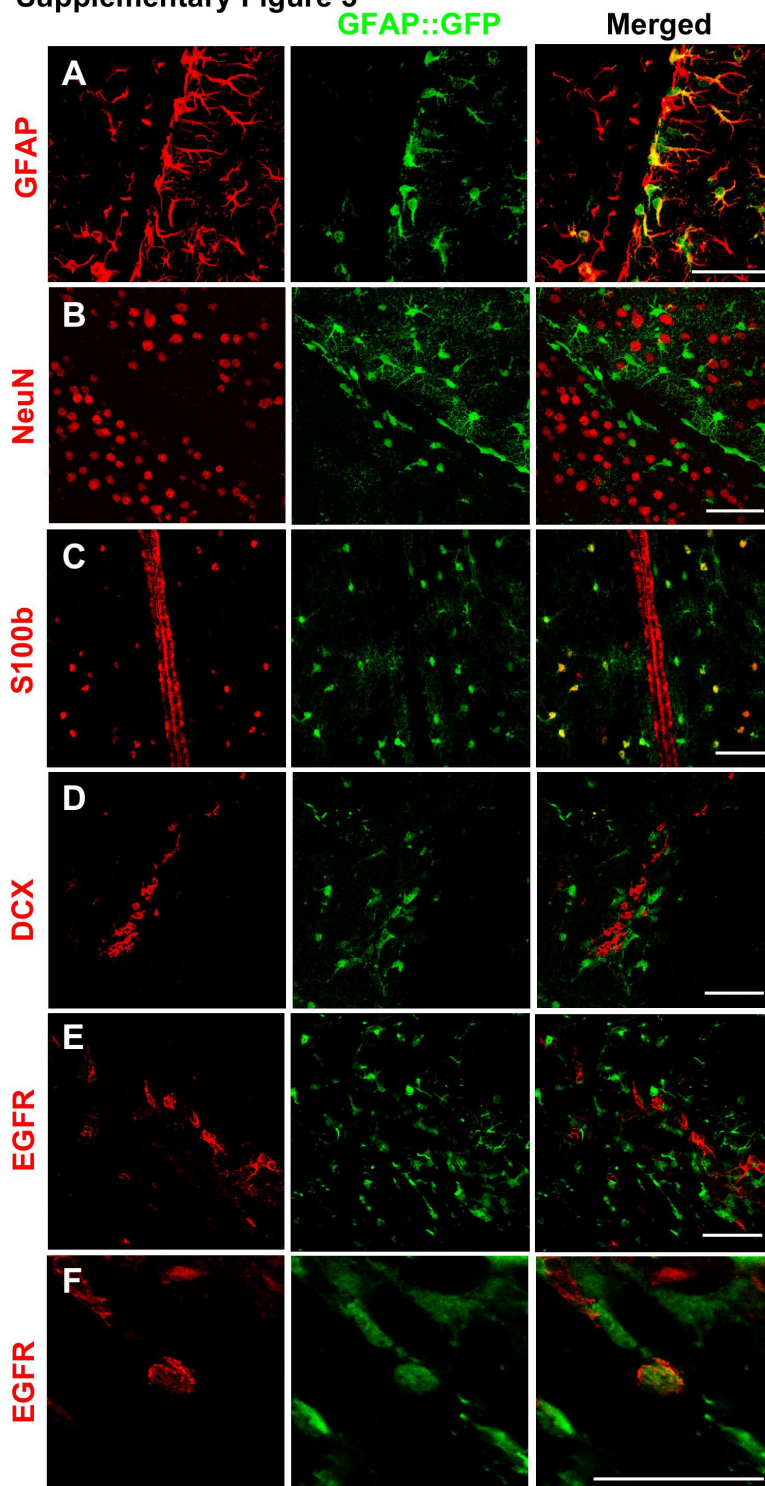


**Figure S3.** Characterization of the adult SVZ in GFAP::GFP mice. GFP (green) is expressed in GFAP positive astrocytes (A), and is not expressed in NeuN positive

neurons (B), or in S100b positive ependymal cells (C). Note that GFP is expressed in S100b positive astrocytes outside of the SVZ. GFP is also not detected in doublecortin (Dcx) positive neuroblasts (D). The majority of EGFR positive cells do not express GFP (E), although a small subset do (F). Note that in other brain regions we observed GFP expression in oligodendrocyte progenitors, which could be due to either a lineage relationship between GFAP+ cells and oligodendrocytes, or non-specific expression in these mice. Scale bars: (A-F) 50  $\mu\text{m}$ .

Supplementary Figure 4

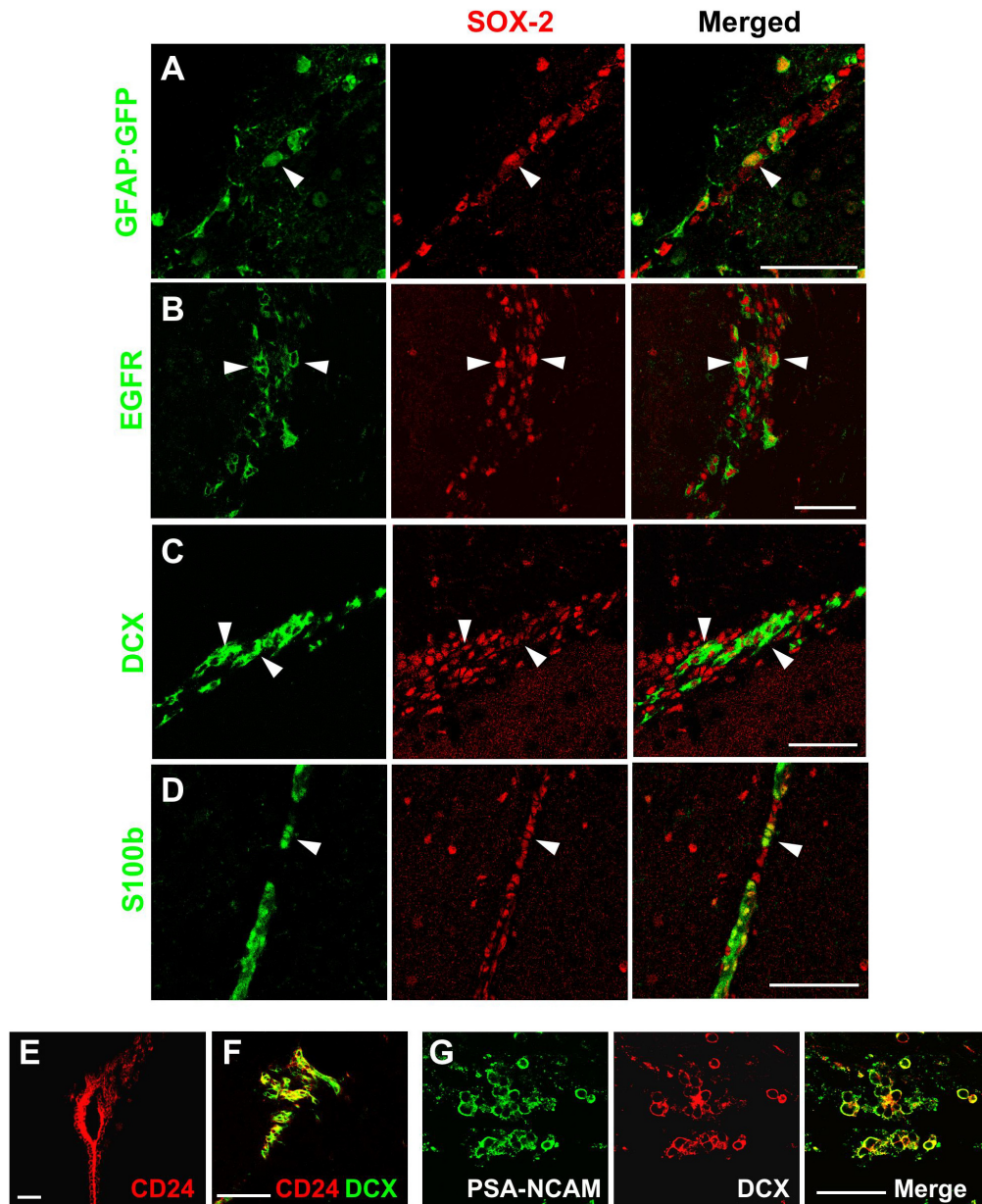


**Figure S4.** Sox2 expression in the adult mouse SVZ. Sox 2 (red) is expressed by all cell types in the SVZ. It is expressed at high levels by (A) GFP-positive astrocytes in GFAP::GFP mice (arrowhead), (B) EGFR positive cells (B, arrowhead) and is expressed at lower levels in Dcx+ neuroblasts (C, arrowhead). It is also expressed in S100b positive ependymal cells (arrowhead, D). (E-G) Doublecortin is expressed in neuroblasts



in the SVZ. Double immunostaining for mCD24 (red), which labels both ependymal cells (E) and neuroblasts (F), and dcx (green). (G) PSA-NCAM (green) expression overlaps with Dcx (red) expression. Scale bars: (A-G) 50  $\mu$ m.

### Supplementary Figure 5

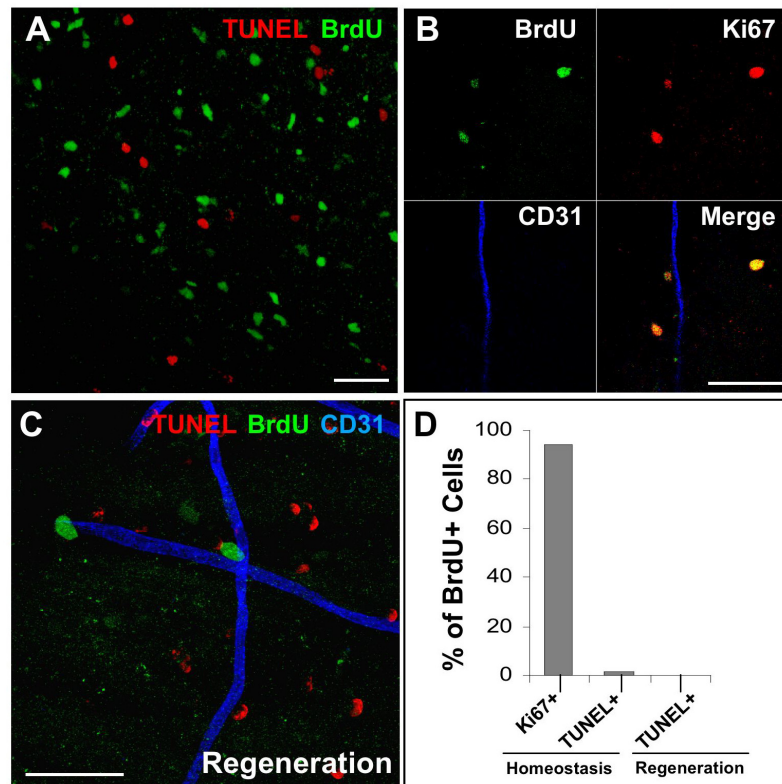


**Figure S5.** Whole mount TUNEL staining of the SVZ during homeostasis (A, B) and regeneration (C). (A) The majority (94.8%) of BrdU positive cells in the SVZ are not TUNEL positive under homeostasis and (94%) are double stained with Ki67. No BrdU positive cells were TUNEL positive 12 hours after cessation of ARA-C treatment. (D) Histogram showing the percentage of BrdU positive cells that are Ki67 positive and TUNEL positive. Scale bars: (A-C) 50  $\mu$ m.

Supplementary Figure 6

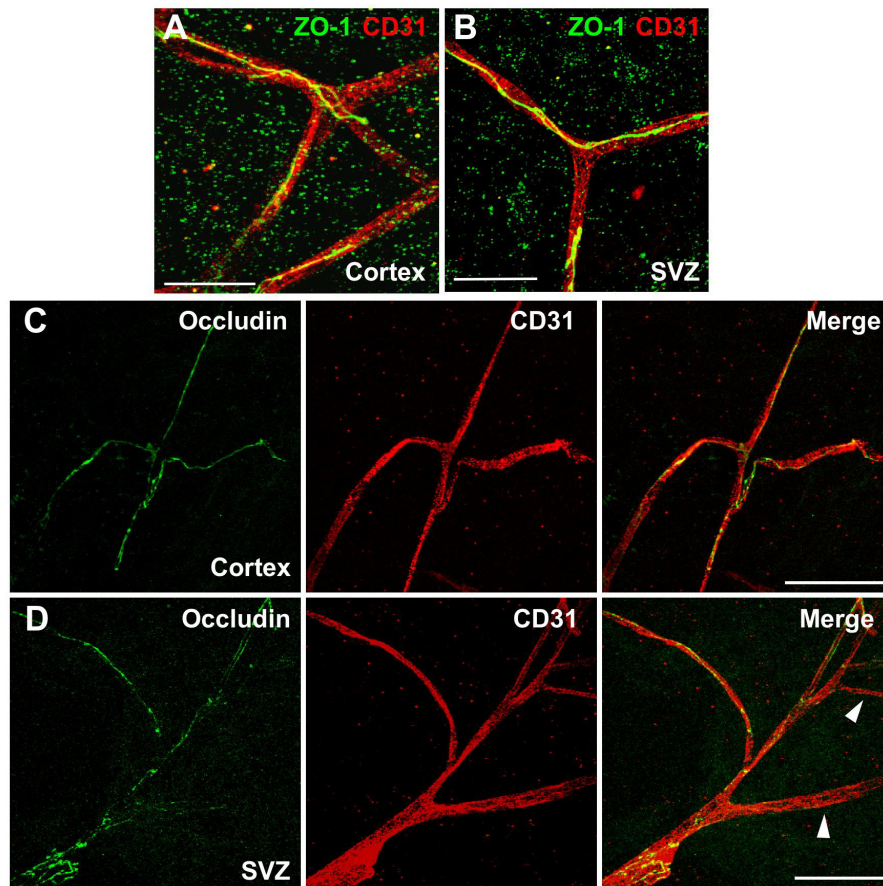


**Figure S6.** Expression of tight junctions in the SVZ. Whole-mounts immunolabeled with CD31 (red) and the tight-junction protein ZO-1 (A,B, green) or Occludin (C, D, green). Tight-junctions are observed in the cortex (A, C) and SVZ (B, D). Some areas along SVZ vessels may lack tight junctions (arrowheads, D). Scale bars: (A, B) 20  $\mu\text{m}$ , (C, D) 50  $\mu\text{m}$ .

Supplementary Figure 7

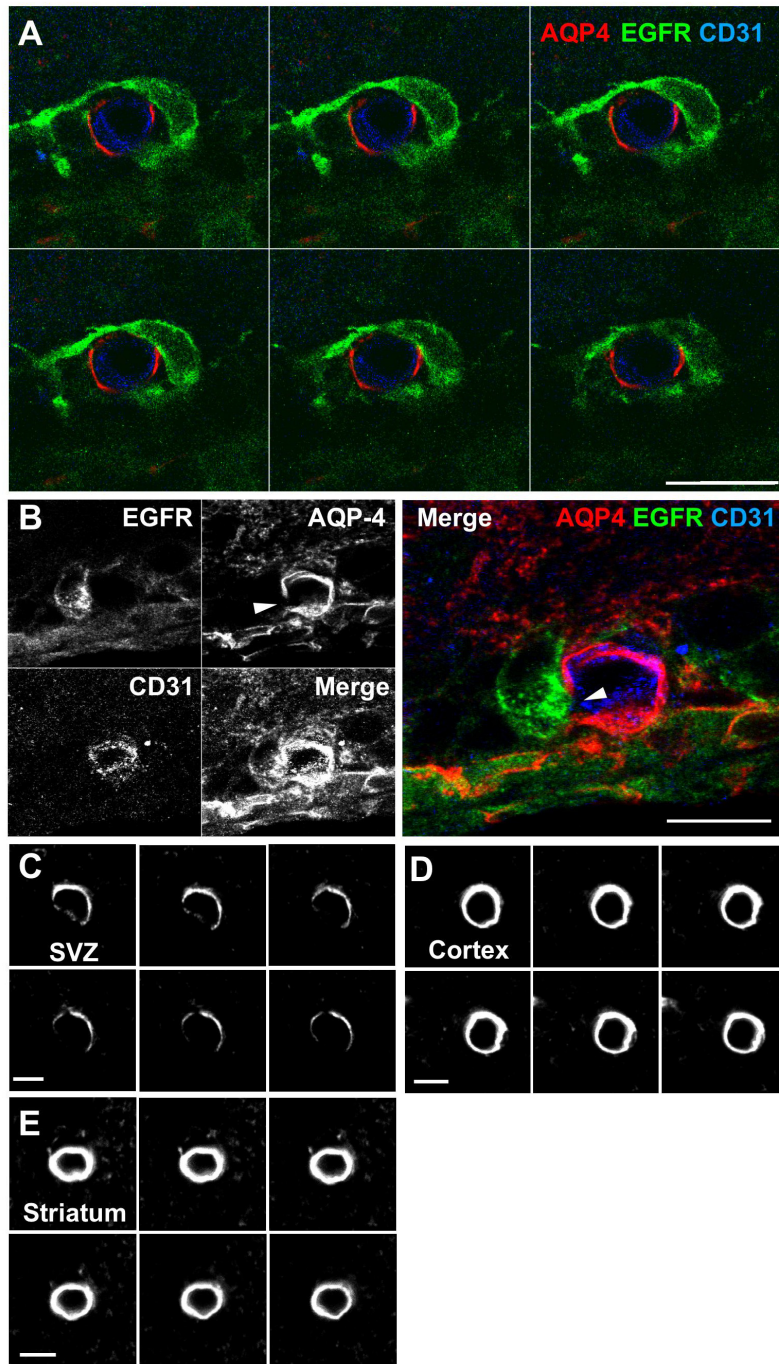


**Figure S7.** (A) Serial 0.5 μm interval optical sections of the cell shown in Figure 5A demonstrating that transit amplifying C-cells (green) contact the vasculature (blue) at regions devoid of AQP-4 staining (red). (B) Another example of an EGFR positive C cell

(green) contacting a CD31 positive blood vessel (blue) at an AQP-4 (red) gap. (C-E) Serial 0.5  $\mu\text{m}$  interval optical sections acquired with identical confocal settings of the blood vessels shown in figure 4J-L, from the SVZ (C), cortex (D) and striatum (E). The vasculature of the striatum and cortex, unlike the SVZ, exhibits a thick layer of AQP-4 staining that completely envelops the outside of blood vessels.

Scale bars: (A, B) 10  $\mu\text{m}$ , (C-E) 5  $\mu\text{m}$ .

### Supplementary Figure 8

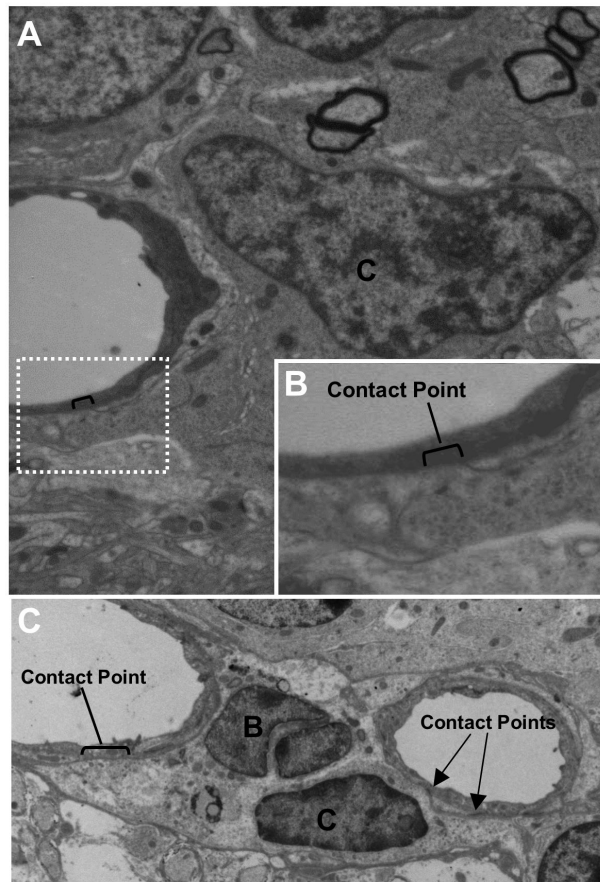


**Figure S8.** (A) EM micrograph showing Type C cell contacting a blood vessel directly (bracket). White dotted box marks area of (B). (B) High magnification view of the contact site. Note that the area of contact for this cell is small. (C) Low power view of cell shown in figure 5C, D showing contact with blood vessels at both ends of the cell.

Supplementary Figure 9

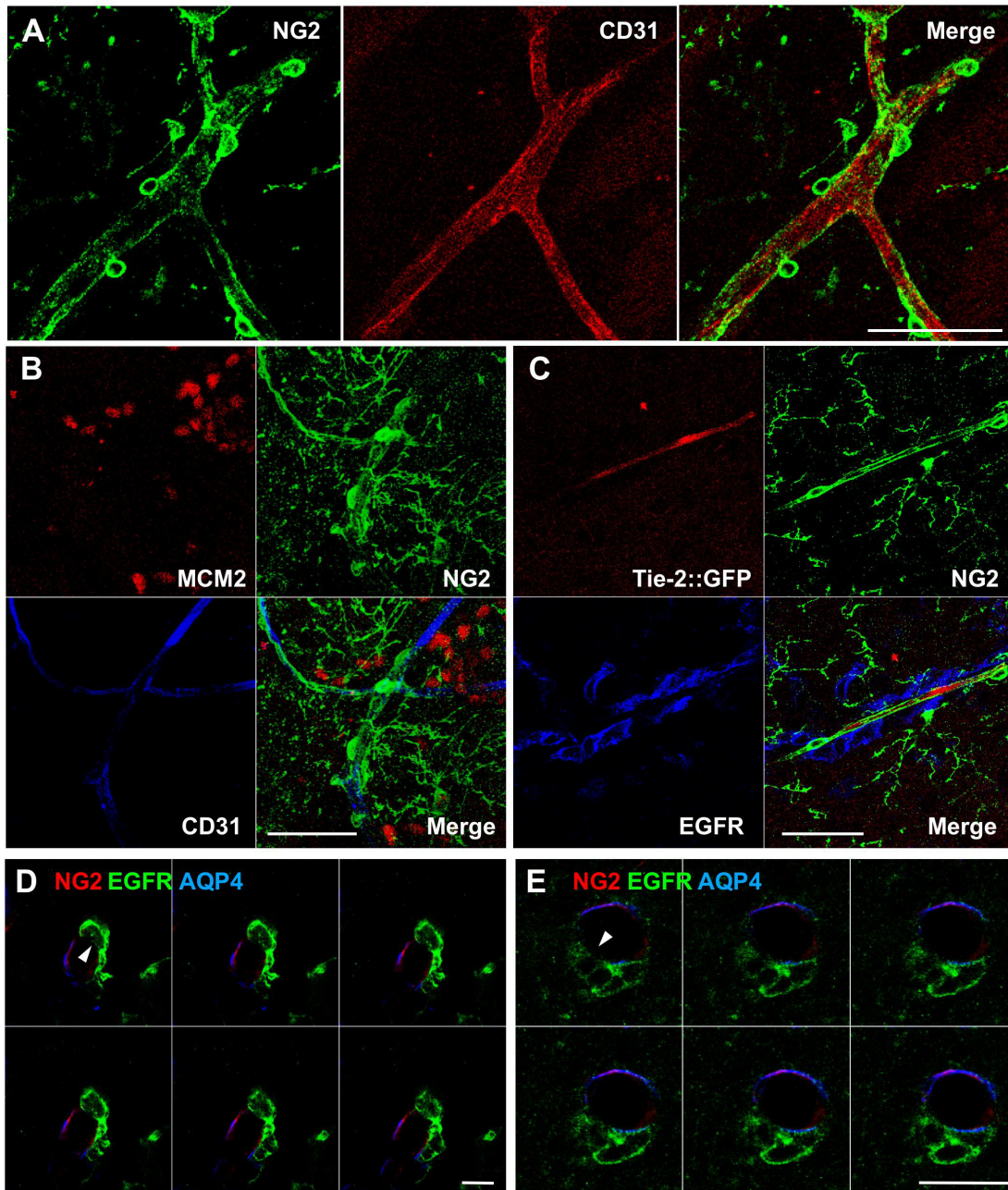


**Figure S9.** EGFR positive transit amplifying C cells contact blood vessels at sites lacking pericyte coverage. (A) Distribution of NG2 positive pericytes (green) along CD31 expressing blood vessels (red) in the SVZ (A). (B) The majority of perivascular NG2 positive cells (96.2%) (green) do not express the cell division marker MCM2 (red).

Dividing pericytes represent 1.6% of dividing SVZ cells. (C) No perivascular NG2 positive cells (green) in TIE-2::GFP mice (endothelial cells in red) were EGFR positive (blue) (D, E) EGFR positive transit amplifying cells contact blood vessels at sites lacking pericyte coverage. (D) Serial 0.5  $\mu\text{m}$  interval optical sections of the cell shown in Figure 6D showing contact of EGFR expressing transit amplifying cell (green) at a region on a blood vessel devoid of both pericyte coverage (red) and AQP4 staining (blue) (arrowhead). (E) Another example of EGFR expressing transit amplifying cells (green) contacting vessels at regions lacking both pericyte coverage (red) and AQP4 staining (blue) (arrowhead). Scale bars: (A-C) 50  $\mu\text{m}$ , (D, E) 10  $\mu\text{m}$ .